AMERICAN SOCIETY FOR MICROBIOLOGY | Microbiology Spectrum

RESEARCH ARTICLE

Patient-Derived Antibody Data Yields Development of Broadly Cross-Protective Monoclonal Antibody against ST258 Carbapenem-Resistant *Klebsiella pneumoniae*

Kasturi Banerjee,[a,b] Michael P. Motley,[a,c] Camila Boniche-Alfaro,[a,b] Somanon Bhattacharya,[a] Raj Shah,[a] Andrew Ardizzone,[a] Bettina C. Fries[a,b,c]

[a]Department of Medicine, Infectious Disease Division, Stony Brook University, Stony Brook, New York, USA
[b]Veteran's Administration Medical Center, Northport, New York, USA
[c]Department of Microbiology and Immunology, Stony Brook University, Stony Brook, New York, USA

Kasturi Banerjee and Michael P. Motley share co-first authorship. Author order was determined by the corresponding author after negotiation.

ABSTRACT The most pressing challenge for the development of anti-capsular antibodies is maximizing coverage against the heterogenous capsular polysaccharide (CPS) of carbapenem-resistant *Klebsiella pneumoniae* (CR-*Kp*). So far, only CR-*Kp* with *wzi154* CPS has been successfully targeted by antibodies. Here, we present murine antibody 24D11, which was developed by vaccinating mice with purified *wzi50*-type CPS. Cross-reactivity and protective efficacy of MAb 24D11 were confirmed against CR-*Kp* that express the 3 most prevalent CPS types (*wzi29*, *wzi154*, *wzi50*) using both *in vitro* and *in vivo* infection models. 24D11 induced complement-mediated and independent opsonophagocytosis in macrophages as well as killing of all CR-*Kp* strains in whole blood cells derived from healthy donors. In a murine intratracheal infection model, 24D11 reduced lung burden and dissemination of CR-*Kp* strains when administered 4 h pre- or postinfection. The protective efficacy of 24D11 remained effective in neutropenic mice. This is the first antibody which exhibits cross-protective efficacy against clade 1 and 2 ST258 CR-*Kp* strains. It overcomes a major barrier to successfully target *wzi29*, a major CPS expressed by ST258 CR-*Kp*. The finding that 24D11 also exhibits potent protective efficacy against *wzi154* CR-*Kp* strains highlights its high potential as a lead agent for the development of broadly active immunotherapy.

IMPORTANCE Here, we present *in vitro* and *in vivo* data for the *wzi50* CPS-specific monoclonal antibody MAb 24D11, demonstrating its cross-protective efficacy against three prominent *win* types (*wzi29*, *wzi154*, and *wzi50*) of the carbapenem-resistant clonal group CG258. In a murine pulmonary infection model, MAb 24D11 reduced bacterial lung burden and dissemination to other organs even if administered 4 h postinfection. Its protective efficacy was also observed in neutropenic mice, which highlights its potential value in clinical settings where oncology patients with CG258 infections may also be neutropenic.

KEYWORDS carbapenem-resistant *Klebsiella pneumoniae*, ST258, anti-bacterial immunotherapy, capsular antibodies, cross-protection, capsular polysaccharide, clade 1 *Klebsiella pneumoniae*

Therapeutic monoclonal antibodies (MAbs) have emerged as the dominant therapeutic modality for treating cancer and immune disorders (1), and more efforts to use them against infectious diseases are emerging (2, 3). These efforts are necessary given the urgency of developing novel treatments to combat multidrug-resistant pathogens, such as carbapenem-resistant *Klebsiella pneumoniae* (CR-*Kp*) infections,

Editor Christopher N. LaRock, Emory University School of Medicine

Address correspondence to Bettina C. Fries, Bettina.Fries@stonybrookmedicine.edu.

The authors declare no conflict of interest. B.C.F. is an attending physician at the U.S. Department of Veterans Affairs (Northport VA Medical Center, Northport, NY). The contents of this study do not represent the views of VA or the US government.

Received 6 June 2022
Accepted 23 June 2022
Published 11 July 2022

which are associated with high mortality even in the most recent SARS-CoV-2 pandemic (4–7). The capsular polysaccharide (CPS) constitutes an important virulence factor of *Klebsiella* that promotes resistance to phagocytosis and serum bactericidal activity. It has been a useful immunogenic target in other organisms (8–10). However, antigenic diversity limits the use of monoclonal antibody as a broader therapy. Numerous *Kp* CPS serotypes exist, which were previously defined by K-serotyping but now are more conveniently and reliably characterized by PCR-sequencing of the capsular adhesion gene *WZI* and other genes within the *cps* locus (11). Interestingly though, CR-*Kp* strains observed in population studies are remarkably clonal, and their prevalent serotypes are limited (5, 12). In the United States, for example, nearly 60% of CR-*Kp* strains belong to clonal group 258 (CG258), and 92% of these clones express one of only four *wzi* alleles (47.9% *wzi154*, also referred to as capsule type KL107; 31.0% *wzi29*, also referred to as KL106; 6.6% *wzi50*; and 6.0% *wzi168*) (5). This restricted prevalence has been relatively stable for the past decade (5, 13–16) although a recent paper (17) reports newly emerging CR-*Kp* strains that belong to CG307.

We and others have successfully developed immunotherapies which target CPS expressed by CG258 strains carrying the *wzi154* allele, which includes the strain responsible for the NIH outbreak (10, 18–23). However, less success has been observed in providing adequate coverage against CG258 strains carrying other *wzi* alleles such as *wzi29* and *wzi50* (18, 19). Because there are few methods for accurately serotyping in the clinical setting, maximizing coverage of all predominant serotypes remains a critical challenge for developing passive immunotherapy.

Recently, we investigated the humoral responses of patients who had convalesced from infection by CR-*Kp* (24). Through this survey, we discovered that polyclonal antibodies of patients infected with *wzi50*-carrying CR-*Kp* demonstrated wide cross-reactivity and protection not only against strains carrying *wzi50*, but against strains carrying *wzi29* or *wzi154* as well. These data suggested that *wzi50* possesses an epitope that elicits cross-protective antibodies to *wzi50*, *wzi29*, and *wzi154* CPS. Informed with these data on patient-derived immune responses, we hypothesized that using *wzi50* as an immunogen might yield cross-reactive and -protective antibodies.

We now present the characterization of a monoclonal antibody (mIgG2b 24D11) which has anti-bacterial activity not only against CG258 strains carrying *wzi50*, but also against *wzi29* and *wzi154* strains. We additionally demonstrate that this antibody can provide cross-protection to mice when given after pulmonary infection, as well as prophylactically. This is the first monoclonal antibody that presents broad activity against dominant *wzi* types expressed by the CG258 strains.

RESULTS

Generation of monoclonal antibody against *wzi50* capsular polysaccharide. With the knowledge that anti-*wzi50* patient antibodies cross-react and protect against other capsular types (24), we utilized *wzi50* as an immunogen to develop novel MAbs. We vaccinated BALB/c mice with unconjugated purified *wzi50* CPS, or with *wzi50* CPS conjugated to *Bacillus anthracis* Protective Antigen (*wzi50-Ba*PA) (Fig. S1A in the supplemental material). Titer responses were poor for both groups of mice, requiring additional booster doses of CPS with adjuvant (incomplete Freud Adjuvant) at 6 and 8 weeks to achieve sufficient titers ($>$1:10,000). This regiment was still insufficient to elicit strong anti-capsular titers in the *Ba*PA-CPS vaccinated mice ($\leq$1:6,400), whereas mice vaccinated with unconjugated *wzi50* reached and maintained high titers ($>$1:10,000) by 6 weeks post-initial vaccination against both *wzi50* CPS and *wzi29* CR-*Kp* bacteria (Fig. S1B).

Splenic fusions with two hybridoma cell lines were screened for activity against *wzi50*, and 3 positive clones with NSO^{bcl2} backgrounds were identified for downstream subcloning and soft agar selection. Of these, we selected and subcloned IgG2b-producing hybridoma 24D11 for further study (Fig. S1A), as it had superior reactivity relative to the other 2 clones. Enzyme-linked immunosorbent assay (ELISA) binding

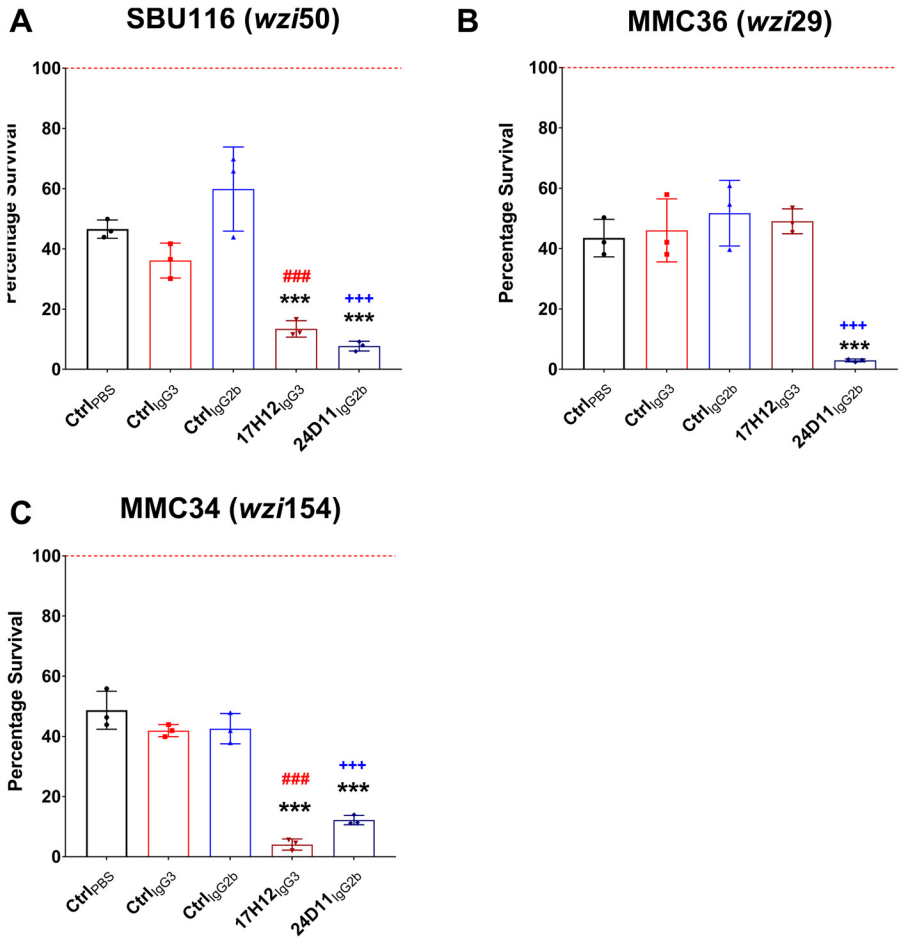

FIG 1 24D11 promotes killing of carbapenem-resistant *Klebsiella pneumoniae* (CR-*Kp*) of multiple serotypes in healthy donor blood. Whole blood samples were treated with an isotype control or with 40 μg/mL of monoclonal antibody (MAb) 24D11 (mIgG2b) or 17H12 (mIgG3) and simultaneously inoculated with 10^5 CFU/mL live CR-*Kp* strains: SBU116, which possesses the *wzi50* allele (A), MMC36, which possesses the *wzi29* allele (B), and MMC34, which possesses the *wzi154* allele (C). CFU/mL/survival values were determined after 1 h in culture and plotted as a percentage of the initial starting inoculum (red dotted line). The experiment was repeated as three separate replicates, with each symbol representing one replicate. For all studies, bars depict means and standard deviations (SD). Overall differences in percent survival between treatment groups (n = 3 per group) were assessed for significance by one-way analysis of variance (ANOVA) with multiple-comparison correction. P values for comparisons between antibody groups and phosphate-buffered saline (PBS), between 17H12 (black *) and its mIgG3 control (red #) and between 24D11 and its mIgG2b control (blue +) are indicated as follows: *, $P < 0.05$; **, $P < 0.01$; ***, $P < 0.001$.

estimated the 50% effective concentration (EC_{50}) of 24D11 against *wzi50* as 4.72 nM (Fig. S1C) and that against *wzi*154 as 5.8 nM, respectively (Fig. S1D).

Anti-*wzi50* antibody 24D11 mediates whole-blood killing of multiple CR-*Kp* strains. To explore the anti-infective potential of MAb 24D11, we examined the antibody-mediated killing of multiple strains of CR-*Kp* in whole blood. As a control, we utilized our previously characterized murine IgG3 (mIgG3) 17H12, developed against CPS of a *wzi154*-carrying CR-*Kp* strain (18). The CFU of all tested CR-*Kp* strains dropped to undetectable levels regardless of condition at 2h. At 1 h, both 24D11 and 17H12 reduced the survival of *wzi50*-carrying SBU116 (~83% reduction in bacterial survival) significantly more than their corresponding control antibodies did ($P < 0.0001$) (Fig. 1A). Interestingly, 24D11 cross-reacted and significantly reduced *wzi29* MMC36 CR-*Kp* bacterial levels in whole blood by 90% ($P < 0.0001$), whereas 17H12 did not significantly affect bacterial levels relative to its control antibody (Fig. 1B). Additionally, both 24D11 and 17H12 promoted the significant killing of *wzi154*-carrying MMC34

(~90% reduction in bacterial survival) compared to their isotype controls ($P < 0.0001$) (Fig. 1C). In addition, we also utilized CR-*Kp* SBU255, a strain belonging to the emerging clonal group CG307 *Kp*, which is genetically distinct from the ST258 clonal group and expresses an unrelated *wzi173* CPS (25), to test the specificity of 24D11. As expected, 24D11 did not promote the killing of both CG307 CR-*Kp* strains (SBU100 and SBU255) in the whole blood assay at 1 h (Fig. S2). Furthermore, we also observed increased cross-reactive killing of MMC34 by 24D11 and of SBU116 by 17H12 relative to the controls (Fig. 1A and C) ($P < 0.0001$). This observation led us to investigate whether both MAbs bind to any conserved epitopes on *wzi50* and *wzi154* CPS by performing modified competitive ELISAs. Binding curves indicated that 17H12 began to compete with 24D11 binding to *wzi50* CPS and *wzi154* CPS at 5 μg/mL, whereas 24D11 began to compete with 17H12 binding to *wzi154* at 10 μg/mL (Fig. S3). These results demonstrate the ability of 24D11 to promote the killing of many different ST258 strains in human blood.

MAb 24D11 promoted cross-protective opsonophagocytosis of multiple CR-*Kp* strains. Macrophages and monocytes are important players in CR-*Kp* clearance, and the antibody-mediated opsonophagocytic uptake by macrophages is important for cell-mediated protection against CR-*Kp* (26–28). Therefore, we investigated the potential of 24D11 to promote opsonophagocytic uptake of different CR-*Kp* strains by the murine macrophage-like cell line J774A.1. Our data showed that 24D11 promoted opsonophagocytosis of 5/6 CR-*Kp* strains, including two *wzi29* strains and one *wzi154* strain (Fig. 2). Three of these five strains required serum for 24D11 to significantly improve opsonophagocytosis relative to the controls (SBU116, MMC34, MMC36), while two strains (MMC38, SBU207) showed serum-independent promotion of opsonophagocytosis. For one strain (MMC38), opsonophagocytosis of CR-*Kp* by 24D11 did not differ with the controls in the presence of serum, with opsonophagocytosis levels equivalent to those in the presence of 24D11 without serum (Fig. 2).

To ensure that the cross-reactivity of 24D11 was dependent on the presence of CPS and not due to nonspecific binding to the bacteria, we tested its ability to promote opsonophagocytosis of CR-*Kp* 33576 (*wzi154*) and its acapsular mutant 33576Δ*wzy* (19) (Fig. S4). 24D11 mediated phagocytosis of the capsular 33576 bacteria but did not promote phagocytic uptake of the acapsular 33576Δ*wzy*. Additionally, when tested against CG307 strain SBU255, 24D11 did not promote phagocytosis of SBU255, as expected (Fig. S4). Taken together, these data confirm that 24D11 enhances phagocytosis of ST258 strains with different polysaccharide capsules.

Intraperitoneal delivery of MAb 24D11 provides cross-protection in intratracheal lung infection model. We followed our *in vitro* observation by exploring the cross-protective efficacy of 24D11 *in vivo* by testing its ability to reduce organ burden in mice intratracheally infected with *wzi50*-, *wzi29*-, or *wzi154*-carrying CR-*Kp* strains. For this investigation, we used our previously utilized pre-opsonized model and a prophylactic model where 24D11 was given intraperitoneally (IP) 4 h prior to intratracheal (i.t.) infection to explore whether 24D11 was able to decrease bacterial lung burden and dissemination in C57BL/6 mice (Fig. 3). Mice injected with 10^6 CFU/inoculum pre-opsonized *wzi50* SBU116 exhibited a moderate 1-$\log_{10}$ reduction in the lung with no effect on the dissemination of the bacteria to the liver and spleen (Fig. 3A). Furthermore, mice infected with 10^7 CFU/inoculum pre-opsonized SBU116 also showed a 1-$\log_{10}$ decrease in bacterial lung burden with no significant reduction observed in bacterial dissemination to the liver or spleen (Fig. 3B). On the contrary, prophylactic administration of 24D11 prior to CR-*Kp* intratracheal infection significantly reduced the lung bacterial burden by 2-$\log_{10}$ and the bacterial spread by 3-$\log_{10}$ for both inoculums of SBU116 ($P < 0.001$) (Fig. 3A and B). Furthermore, at a high-inoculum dose of SBU116, we observed better lung CR-*Kp* clearance as well as inhibition of bacterial dissemination in 3 out of 6 mice within the pre-treated group compared to that in the pre-opsonized group (Fig. 3A and B). In mice infected with 24D11-opsonized *wzi29* MMC36 strain (Fig. 3C) and *wzi154* MMC34 strain (Fig. 3D), we observed more significant CFU reductions of 3 and 2 $\log_{10}$-fold in lung tissue, respectively. Furthermore, a moderate drop

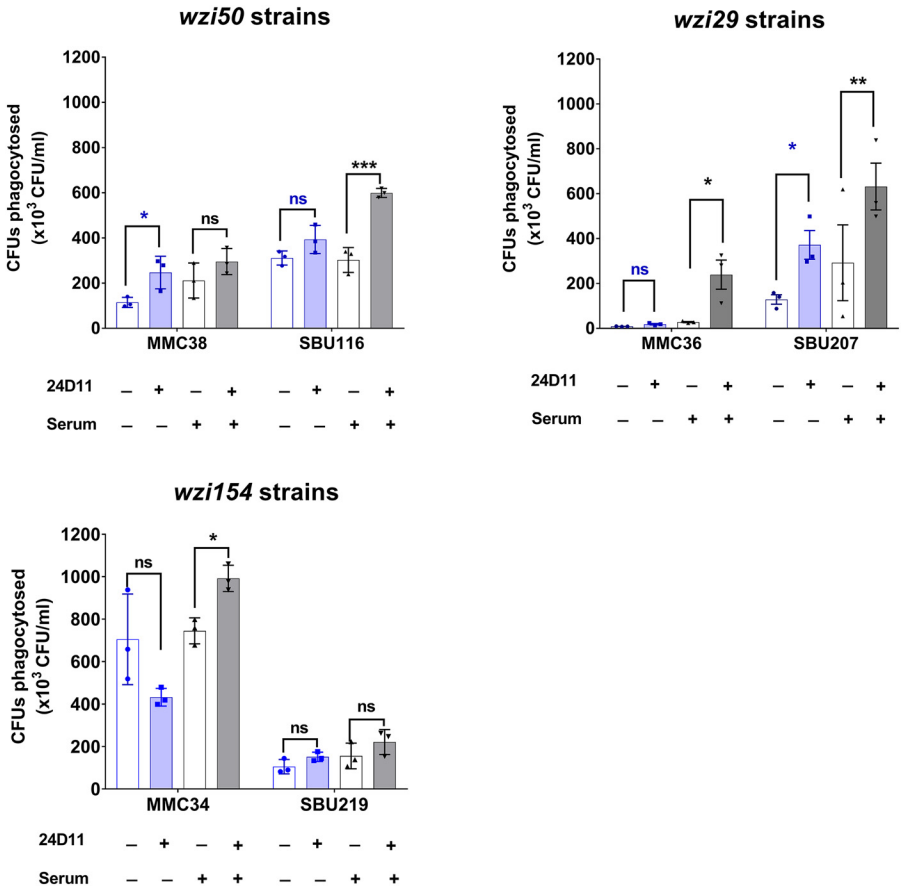

FIG 2 24D11 promotes macrophage-mediated opsonophagocytosis of CR-*Kp* strains across several *wzi* types. Opsonophagocytic uptake by J774.A1 murine macrophage-like cells of *wzi50* strains (MMC38 and SBU116), *wzi29* strains (MMC36 and SBU207), and *wzi154* strains (MMC34 and SBU219), pre-opsonized with or without 24D11, was measured after 1 h in the presence or absence of normal human serum (NHS). The CFU phagocytosed was calculated as the number of CFU recovered after washing and macrophage lysis. Bars depict means and SDs of three independent experiments, with wells performed in triplicate. Differences between the non-serum treated group with or without 24D11 (blue *) and differences between the NHS-treated group with or without 24D11 (black *) were assessed for significance by repeated-measures two-way ANOVA, with the results of a Tukey's *post hoc* test for multiple comparisons shown in the graph. *P* values are indicated by ns (not significant), $P \geq 0.05$; *, $P < 0.05$; **, $P < 0.01$; and ***, $P < 0.001$.

in the bacterial load in the liver and spleen in antibody-opsonized MMC36- and MMC34-infected mice was observed (Fig. 3C and D). Pre-treatment with 24D11 had similar effect on the reduction of lung bacterial burden, but for both MMC36 (Fig. 3C) and MMC34 (Fig. 3D), almost all animals showed significant inhibition in bacterial dissemination compared to their pre-opsonized counterparts (Fig. 3C and D).

Next, we investigated whether 24D11 also protected CR-*Kp* infected mice if administered intraperitoneally 4 h post-surgery (Fig. 4). To better mimic clinical therapy, we treated CR-*Kp* infected mice 4 h after i.t. infection. These data demonstrated a significant drop of 3 $\log_{10}$-fold in the lung burden of SBU116 CR-*Kp* infected mice compared that in the control groups (Fig. 4A). In addition, SBU116-infected mice treated intraperitoneally with MAb 24D11 showed a moderate 1-$\log_{10}$ reduction in the bacterial CFU disseminated to other organs (Fig. 4A). For MMC29 (*wzi29*)- and MMC34 (*wzi154*)-infected mice, IP treatment with 24D11 post-i.t. surgery also demonstrated a significant decrease in the bacterial organ load in lungs (Fig. 4B and C). Furthermore, IP treatment with MAb 24D11 prevented dissemination to the limit of detection to liver and spleen in 3 out of 5 MMC36-infected mice (Fig. 4B) and reduced bacterial spread to other affected organs in MMC34-infected mice (Fig. 4C). In summary, these murine

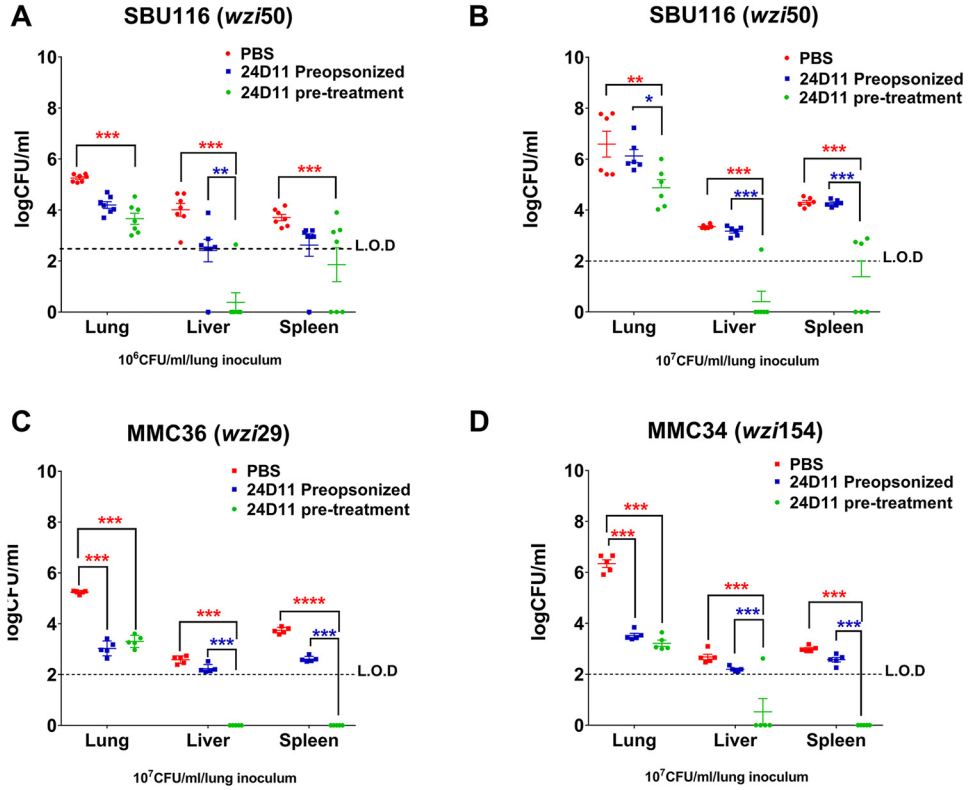

FIG 3 24D11 exhibits potent protective efficacy in CR-*Kp* pulmonary infection when given prophylactically. Organ burden was measured in mice 1 day after infection with SBU116 (A and B), MMC36 (C), or MMC34 (D) strains at the indicated inoculums in the presence or absence of 24D11, either as a pre-opsonization mix with the bacterial prior to infection (40 μg/mL final concentration, blue squares) or as a prophylactic intraperitoneal dose 4 h prior to infection (10 mg/kg, green circles). Symbols represent individual mice pooled from a single experiment, and bars represent means and SD. Differences between CFU between treatment groups were compared for significance by one-way ANOVA, with results of Tukey's *post hoc* test for multiple comparisons displayed in the graph. Red asterisks indicating significant CFU differences to PBS, or blue asterisks indicating significant CFU differences between treatment groups, are shown if *P* values were below 0.05 (*), 0.01 (**), or 0.001 (***).

experiments demonstrate that 24D11 also exhibits cross-reactive efficacy *in vivo*. In addition, 24D11 can be used as a prophylactic a well as a therapeutic reagent.

CR-*Kp* lung clearance is improved by MAb 24D11 in neutropenic mice. Previously published data showed that 17H12 could promote clearance of MMC34 from the lung in neutropenic mice (29). Therefore, we tested whether MAb 24D11 was also protective

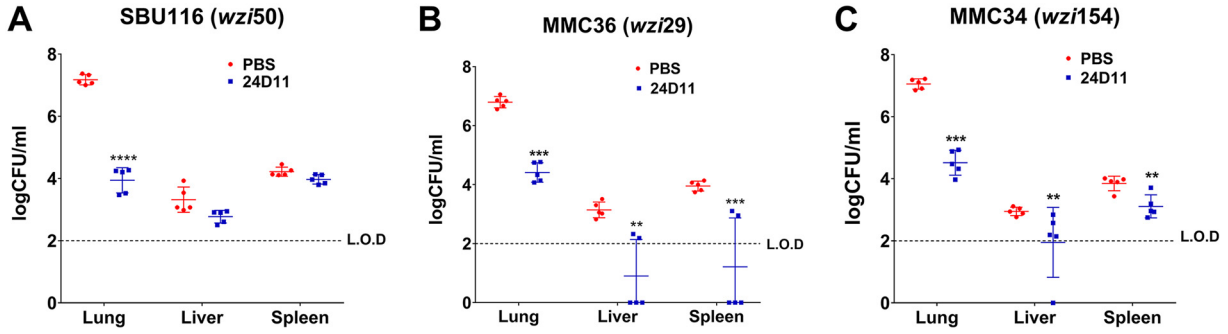

FIG 4 24D11 protective efficacy persists when given postinfection. Organ burden was measured in mice 1 day after infection with 100 μL of 10^8 CFU/mL of SBU116 (A), MMC36 (B), or MMC34 (C) strains and then treated with intraperitoneal administration of PBS or 24D11 (10 mg/kg) 4 h after infection. Symbols represent individual mice pooled from 2 individual experiments performed on two separate days. Bars represent means and SD. Differences between PBS group and 24D11 postinfection treatment groups for SBU116, MMC36, and MMC34 were compared and assessed for significance by multiple *t* tests (one unpaired *t* test per organ between two groups) with false discovery rate at 1%, as displayed in the graph. Asterisks indicate significant CFU differences if *P* values were below 0.05 (*), 0.01 (**), 0.001 (***), or 0.0001 (****).

in neutropenic mice infected with SBU116 CR-*Kp* strain. Ly6G-mediated neutrophil depletion and generation of neutropenic mice was confirmed by flow cytometry (Fig. 5A). Our data showed that mice depleted of neutrophils with Ly6G and infected with SBU116 (10^6 CFU/inoculum) exhibited a higher bacterial lung burden compared to immunocompetent untreated and antibody-treated mice (Fig. 5B). Intraperitoneal treatment with MAb 24D11 decreased the bacterial burden in the lung tissue in both immunocompetent and neutropenic mice by more than 100-fold relative to the untreated controls (Fig. 5B). 24D11 treatment also prevented dissemination in all immunocompetent mice, but not in neutropenic mice (Fig. 5B). MAb 24D11 had no effect in neutropenic mice when a higher inoculum was used (Fig. S5 in Text S1).

To better understand the immune cells involved in mediating the anti-infective efforts of 24D11, we studied and compared innate immune cells in both immunocompetent and neutropenic mice (Fig. 5C and Fig. S6 in Text S1). First, we observed and confirmed >80% depletion of neutrophils (black box) in Ly6G-treated mice (Fig. 5C). $CD45^+$ cells were further subtyped. Immunophenotyping of the innate cells showed no difference in the population of M1 macrophages, but a significant change in M2 macrophage population was observed (Fig. 5C). Interestingly, neutropenic mice exhibited higher numbers of M2 macrophages in lung tissue, which was decreased by 24D11 treatment of neutropenic mice to values similar to those observed in the immunocompetent mice. Furthermore, in the lungs of neutropenic and wild-type mice, MAb treatment increased the presence of inflammatory monocytes (Fig. 5C). Non-classical resident monocytes were increased by 47% in neutropenic mice relative to the immunocompetent mice but were not affected by MAb treatment (Fig. 5C). We observed no change in $CD45^+CD3^+$ T cell populations across all experimental groups (data not shown). Additionally, we investigated the cytokine levels of interleukin (IL)-17 and tumor necrosis factor alpha (TNF-α) and observed a decrease between immunocompetent versus neutropenic mice, but no difference was reported within both groups when they were treated with phosphate-buffered saline (PBS) or 24D11 (Fig. 5D and E). In summary, protective efficacy of MAb 24D11 was still observed in neutropenic mice infected with SBU116 and was associated with lower recruitment of M2 macrophages to infected lung tissue.

24D11 monotherapy has the same efficacy compared to 17H12 and 24D11 combination therapy against *wzi154* CR-*Kp* infection. Because we had observed binding competition between 24D11 and 17H12, we sought to determine how this interaction would affect opsonophagocytosis and *in vivo* efficacy if they were given together. We tested whether a combination of the two MAbs promoted effectiveness in clearing *wzi154* CR-*Kp* intratracheal infection. First, we explored whether phagocytic uptake by macrophages was enhanced when 24D11 and 17H12 were combined. We found that the combination therapy in the absence of serum increased opsonophagocytis relative to PBS treatment, but not relative to 17H12 treatment alone (Fig. 6A, left panel). We also found that although both 17H12 and 24D11 promoted opsonophagocytosis in the presence of serum, the combination of the two MAbs did not further enhance phagocytosis (Fig. 6A, right panel).

In an intratracheal lung infection model, we observed that MMC34-infected mice treated intraperitoneally with 17H12 and 24D11 (10 mg/kg/antibody) combined therapy had a significant drop in the organ burden load and a drop in dissemination by >3 $\log_{10}$-fold (Fig. 6B) which was slightly higher than the 2.5 $\log_{10}$ achieved. We found that 17H12 alone had a limited effect on reducing bacterial spread to liver and spleen (Fig. 6B) whereas 24D11 monotherapy prevented dissemination to other organs, which was not further enhanced by the combination of 24D11 with 17H12 (Fig. 6B). We repeated the opsonophagocytosis study with SBU116 CR-*Kp* strain, and only bacteria pre-opsonized with 24D11, whether alone or in combination, were phagocytosed by macrophages under both conditions. No difference in phagocytosed CFU was observed between the 24D11 monotherapy and combination therapy groups (Fig. S7 in Text S1). These data indicate that the protective efficacy of monotherapy with

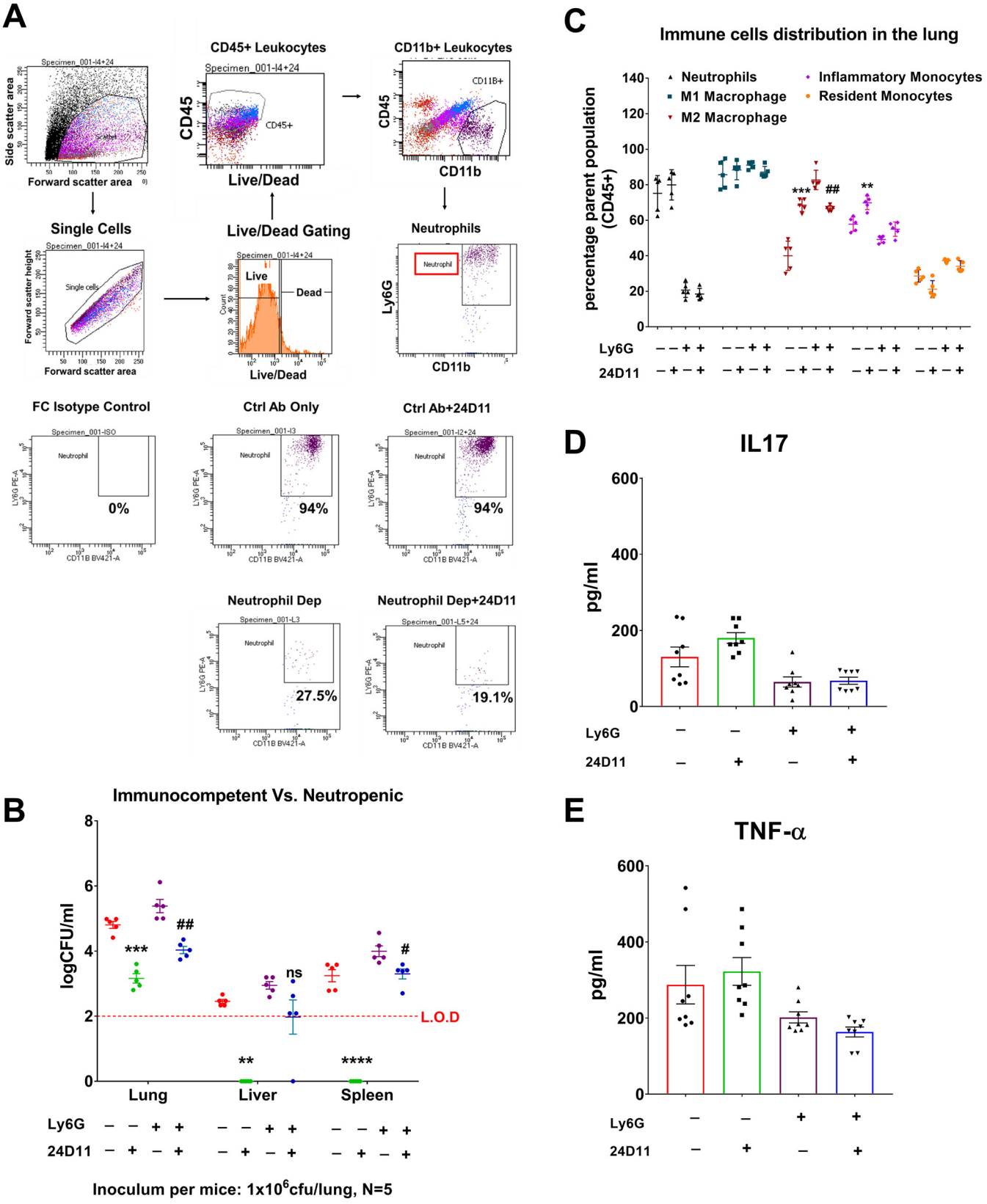

FIG 5 24D11 exerts anti-CR-*Kp* efficacy in neutropenic mice. (A) Cells were gated in side scatter area (SSC-A) and forward scatter area (FSC-A) dot plots to eliminate dead or aggregated cells. Single cells were gated in a forward scatter height (FSC-H) versus FSC-A dot plot to eliminate doublets. Single cells were then gated on a Live/Dead Alexa 700 Axis to eliminate dead cells: $CD45^+$ live leukocytes were gated. $CD45^+CD11b^+$ leukocytes were gated and $Ly6G^+$ gating on $CD11b^+$ leukocytes was chosen to analyze neutrophils. Flow cytometry isotype control showing 0% of cells in the $Ly6G^+$ Neutrophils

(Continued on next page)

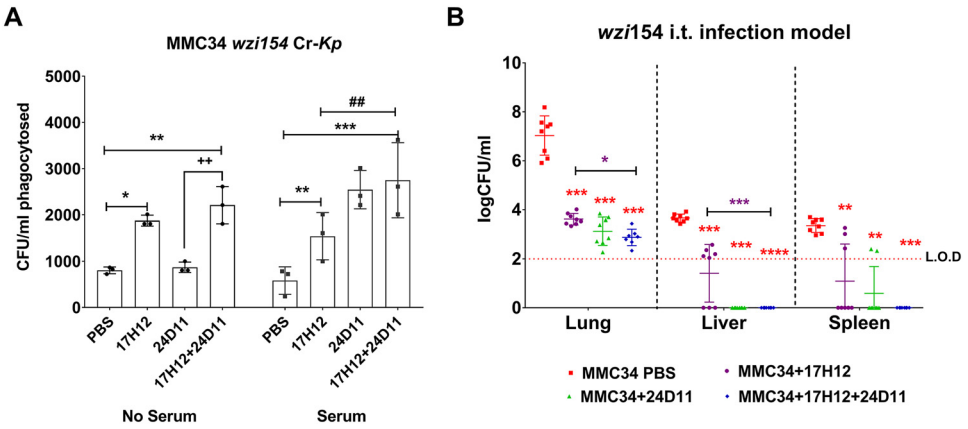

FIG 6 Combining 24D11 and 17H12 does not further enhance protective efficacy against *wzi*154 CR-*Kp*. (A) Phagocytosis of *wzi154* MMC34 by J774.A1 murine macrophage-like cells after incubation with 40 μg/mL of either 24D11, 17H12, or the combination of both antibodies with and without normal human serum. Bars depict means and SDs of three independent experiments, with wells performed in triplicate. Differences between PBS and other treatment groups (*) with or without serum, differences between 24D11 and combination group with or without serum (+), and differences between 17H12 and combination group with or without serum (#) were assessed for significance by repeated-measures two-way ANOVA with results of Tukey's *post hoc* test for multiple comparisons displayed in the graph. *P* values are indicated as ns, $P \geq 0.05$; *, $P < 0.05$; **, $P < 0.01$; and ***, $P < 0.001$. Bacterial burdens in lungs, livers, and spleens of mice infected with 1×10^8 CFU/mL inoculum of MMC34 and intraperitoneally treated with 40 μg/mL of either 24D11, 17H12, or both in combination 4 h post-surgery (B). Differences in CFU within treatment groups were assessed for significance by two-way ANOVA. Individual comparisons made within treatment groups were tested using Tukey's *post hoc* test with *P* values displayed in the graph. *P* values in red indicate comparison between wild-type and antibody-treated mice; *P* values in purple indicate comparison between 17H12-treated mice and 24D11- or combination-treated mice. Each dot represents one mouse. Data are shown as mean ± SD and *P* values are shown as ns, $P > 0.1$; *, $P < 0.05$, **, $P < 0.01$; ***, $P < 0.001$; and ****, $P < 0.0001$.

24D11 is not further enhanced by combining it with 17H12 therapy. It also confirms that 24D11 has potent efficacy against a *wzi154*-carrying clade 2 CR-*Kp* strain.

DISCUSSION

The antigenic variability of the CPS of *K. pneumoniae* remains the primary obstacle to developing immune therapies against it. Based on previous studies, the antigenic diversity of CR-*Kp* ST258 CPS appears restricted to only a few *wzi* types (*wzi154*, *wzi29*, *wzi50*, *wzi168*) which are expressed by the majority of CR-*Kp* strains (5, 12, 13, 30, 31). Such restriction is an opportunity to develop immunotherapies for treating the most drug-resistant CR-*Kp* strains, for which there is little recourse should infection occur. While we and others have successfully targeted *wzi154* CPS through vaccines and MAbs (18, 19, 32), there had previously been no success in targeting *wzi29* CPS. The observation of cross-reactivity against *wzi29* and *wzi154* by serum antibodies from patients who convalesced from infection with *wzi50*-expressing ST258 (24) led us to hypothesize that those cross-reactive epitopes on *wzi50* could be leveraged to provide broad protection against ST258 strains. The success of this approach highlights the importance of a detailed analysis of human antibody responses. The sugar compositions

FIG 5 Legend (Continued)
gate. Percentage neutrophils from each treatment group are shown in the Ly6G$^+$ Neutrophils gate. (B) Bacterial burden in the lungs of C57BL/6 mice depleted of neutrophils (Ly6G) or administered a control antibody and subsequently infected with 100 μL of 1×10^8 CFU/mL inoculum of SBU116, with or without post-surgical treatment with 24D11 (10 mg/kg). Immunophenotyping of immune cells engaged in CR-*Kp* clearance from lungs of the control neutropenic mice using flow cytometry and analyzed by BD FACSDiva and Flowing Software, with gating scheme demonstrated in Fig. S6 in the supplemental material (Text S1). Immune cells are depicted in the graph as follows: neutrophils, black triangle; M1 macrophages, greyish blue squares; M2 macrophages, maroon inverted triangle; inflammatory monocytes, purple diamond; resident monocytes, yellow circles (C). Measurement of cytokines interleukin-17 (IL-17) (D) and tumor necrosis factor alpha (TNF-α) (E) was performed using a BioLegend ELISA Max Deluxe set (cat no. 436204 and 430904). For all studies, overall differences in CFU, percentage population, and cytokine levels between treatment groups and neutrophil statuses were assessed for significance by two-way ANOVA. Individual comparisons made within the wild-type (* symbols) or neutropenic (# symbols) groups of mice with or without 24D11 treatment were tested using Tukey's *post hoc* test, and the *P* values are displayed in the graph. *P* values shown in asterisks (*) depict comparison within the wild-type group with or without 24D11 treatment and those shown as # depict comparison within the treatment groups of mice with the same neutrophil status. Data are shown as mean ± standard error of the mean. ns, $P > 0.1$; *, $P < 0.05$; **, $P < 0.01$; ***, $P < 0.001$; and ****, $P < 0.0001$.

of *wzi29* and *wzi50* (13) are very different, and the precise chemical structures of the cross-reactive epitopes have yet to be elucidated. Also, mice vaccinated with *Bacillus anthracis* protective antigen (BaPA)-conjugated *wzi50* CPS did not mount high Ab titers, suggesting that protein conjugation disrupted antigenic epitopes (33).

We now present the anti-*wzi50* mIgG2b antibody 24D11, which has significant *in vitro* and *in vivo* activity against both cognate and noncognate ST258 strains. Bactericidal activity in the whole blood was improved by 24D11 against *wzi50*, *wzi*29, and *wzi154* strains, suggesting broad cross-coverage activity despite being raised against a single capsular polysaccharide. Similarly, 24D11 also improved opsonophagocytosis of several *wzi50*, *wzi154*, and *wzi29* strains. Some strains were opsonized by serum irrespective of antibody (such as MMC38), whereas others required antibody-mediated complement deposition for effective phagocytosis (SBU116) (19). This finding is consistent with previously described variability in complement dependence among CR-*Kp* strains expressing the same *wzi* type CPS (13, 19). Additionally, serum may exhibit bactericidal activity before opsonophagocytosis, which could affect final phagocytosis counts. More studies are needed to elucidate whether 24D11 also induces capsule shedding, which has been described for capsule-specific antibodies of *Streptococcus pneumoniae* (34).

We also demonstrated the activity of 24D11 against *wzi50*, *wzi154*, and *wzi29 in vivo* with reductions in the lung bacterial burdens of certain CR-*Kp* strains when bacteria were pre-opsonized with MAb. Systemic administration of 24D11 reduced bacterial burdens in the lungs and dissemination to other organs for all tested strains when given prophylactically. Most importantly, the potent efficacy of 24D11 was maintained when it was given therapeutically 4 h after infection. Hence, 24D11 demonstrates efficacy against CR-*Kp* even if administered after the establishment of infection. To date, only a few studies have shown antibody efficacy against multidrug-resistant *Kp* when antibody is administered 1 h postinfection (35–37). Additionally, these data confirm that 24D11 does not solely act through simple steric inhibition or inactivation, which cannot be ruled out in the pre-opsonization model (18, 24, 29). As opposed to the ST23 *Klebsiella* stains, ST258 strains are not very virulent in mice, and lethality is only achieved with high inocula and occurs within 24 h, most likely because of LPS intoxication, which does not mimic human disease. This limitation is an established challenge in the field and therefore efficacy of Abs is usually demonstrated by assessing the clearance of bacterial burden in the lung of mice and primates (28, 32, 38, 39).

The finding that 24D11 also exhibits protection in neutropenic mice is very encouraging for clinical development, since this CR-*Kp* infection commonly occurs in immunocompromised neutropenic patients with hematologic malignancies who are at high risk for poor outcomes (40). In both undepleted and neutropenic mice, cytology data demonstrate the ability of 24D11 to promote recruitment of inflammatory monocytes, which have been previously shown to contribute to CR-*Kp* clearance (28). This recruitment, combined with the successful reduction of bacterial burdens in the lungs of neutropenic mice treated with 24D11, further emphasizes a role for these cells. Additionally, the effect of our antibody on the population of anti-inflammatory M2 macrophages appears to change based on the presence or absence of neutrophils, with 24D11 promoting M2 recruitment in the presence of neutrophils but reducing them in the neutropenic state. Certain CR-*Kp* stains have been previously shown to influence NF-$\kappa\beta$ and STAT-6 signaling to promote anti-inflammatory M2 polarization to enhance colorectal tumorigenesis and recruit monocytic myeloid-derived suppressor cells which allow prolonged survival within the infected lung (39, 41), suggesting an anti-inflammatory role of CR-*Kp* in promoting its survival. IL-10, produced by myeloid-derived suppressor cells, has also been shown to be crucial for the host defense against CR-*Kp* (42). Due to sample constraints, we were only able to measure TNF-α and IL-17 levels, which were not affected by 24D11.

Before the discovery of 24D11, we had posited that any CPS-specific MAb therapy strategy against CG258 CR-*Kp* would require a cocktail of two or more, since data on our 17H12 antibody and data by other colleagues suggested a divide between immune recognition of *wzi154* CPS epitopes and *wzi*29 CPS epitopes (18, 19). Our *in*

vitro and *in vivo* data demonstrated that in most cases, treatment with 24D11 was not inferior to combination treatment with the *wzi154*-CPS-specific antibody 17H12. This may be due to a shared epitope of 24D11 and 17H12, as indicated by competition ELISAs. The destruction of immunogenic epitopes during the purification of the *wzi*29 CPS (19, 24) was likely the underlying cause of failed attempts to generate monoclonal Abs to this capsule type in the past, and also prevents us from determining the affinity of 24D11 for the CPS. We therefore measured Ab against *wzi*29-expressing CR-*Kp*. Improved purification models of CPS may allow more accurate affinity measures in the future.

Antibody therapies have finally emerged as major potential therapeutics for infectious diseases through their successful use in the coronavirus pandemic (43). Passive immunotherapy has the potential to be a useful tool against multidrug-resistant organisms, especially in individuals who lack a strong immune response (44, 45). The difficulty of these therapies involves ensuring that the antibody is effective against the target, since organisms such as *Klebsiella* have extensive capsular variability and empirical therapy with MAbs is not cost-conducive (46–48). Studies have also shown that many CR-*Kp* infections occur most frequently in colonized individuals, and usually with strains congruent with their colonizing flora (49). Thus, an anti-CG258 antibody could possibly be used in patients who have been identified as carriers of the infection through perianal, fecal, and nasal screening and molecular testing for multilocus sequence typing and *wzi* allele carriage, although continued development of faster diagnostic tools would be beneficial (50). Additionally, based on the efficacy of 24D11 and the predominance of *wzi154*, *wzi29*, and *wzi50* strains within CG258 in the US, this antibody could potentially be active against 70 to 100% of ST258 strains, which constitute the majority of CR-*Kp* isolates in the US according to recent reports (5, 13, 30, 51).

However, the newly emerging GC307 strains would not be covered by this monoclonal antibody. Their *wzi*174 capsule type does not bind 24D11. The structure of the cross-protective epitopes of *wzi50* has not been elucidated. Although the sugar composition of *wzi50* is distinct from those of *wzi29* and *wzi154*, linkage analysis and investigations with glycan arrays may help identify conserved cross-protective epitopes. Bioconjugate strategies suggest the possibility of generating immunogenic CPS without labor-intensive purification which may also damage the native sugar architecture (52). The evolution of CG258 is marked by numerous recombinations of the CPS region and multiple insertion sequence (IS) elements within the loci (31, 53). Such elements could facilitate recombination and lead to diversification of the capsule, which occurred after the initial success of pneumococcal vaccines (54). Hence, vaccine strategies against *Klebsiella* could introduce selective pressure on the ST258 capsule. Transient treatment with CPS-specific MAbs, on the other hand, would not have a selective effect. Administering MAbs in combination with antibiotics to immunocompromised patients who are colonized and require aggressive chemotherapy may be more successful than a vaccination-based approach.

In summary, our data suggest that the anti-*wzi50* MAb 24D11 potentially provides broad protection against three prevalent *wzi* types of carbapenem-resistant *Klebsiella pneumoniae*, with preserved efficacy in neutropenic mice. This information will support and promote future work on the development of CPS-based vaccines.

MATERIALS AND METHODS

Ethics statement. Animal study protocols were approved by the Animal Committee (IACUC) at SBU (approval no. 628253). Healthy donors consented with Institutional Review Board (IRB)- and SBU Human Subjects Committee-approved protocols and gave blood donations under IRB no. 718744. No potentially identifiable human images or data are presented in this study.

Capsular polysaccharide purification and conjugation. Capsular polysaccharide from carbapenem-resistant *K. pneumoniae* strain MMC38 (*wzi50*) was purified according to the methods of Banerjee et al. (24) and detailed in the Methods section in Text S1 in the supplemental material. Conjugation to the protective antigen of *Bacillus anthracis* (*wzi50*-BaPA) using the l-cyano-4dimethylaminopyridinium tetra-fluoroborate (CDAP) method was performed as previously described (55).

Vaccinations and titer calculations. BALB/c mice (Taconic) were administered either 10 μg of BaPA-conjugated *wzi50* CPS, unconjugated *wzi50* CPS, or no polysaccharide in 100 μL of a 1:1 mixture of

PBS with Complete Freund's Adjuvant by intraperitoneal injection (13, 56). Booster injections were given using a 1:1 mixture of Incomplete Freund's Adjuvant until sufficient titers (1:10,000) were reached. Serum titers in mice were measured from clotted serum extracted by facial bleed using ELISA with plates coated with unconjugated *wzi50* CPS and conjugated *wzi50* CPS, and also against methanol-fixed whole CR-*Kp* bacteria, as per protocol (24, 52). Serum titer was defined as the lowest serum dilution at an optical density (O.D.) of vaccinated mouse serum of $\geq$2.5 times the O.D. of naive mouse serum.

Monoclonal antibody generation and purification. Fusion and cloning were performed as described previously (56) using polyethylene glycol-mediated fusion of splenocytes collected 2 weeks after the final booster with unconjugated *wzi50* CPS to myeloma lines Ag.8 or NSO^{bcl2}, followed by selection in hypoxanthine-aminopterin-thymidine (HAT) medium. Details on cloning and selection of positive hybridomas and antibody production are described in the Methods S2 section of Text S1. Antibodies were produced weekly over 6 months and were purified using Pierce Protein G Affinity Chromatography per the manufacturer's protocol and then concentrated by centrifugal filtration (AMICON 30K), filter-sterilized, snap-frozen in liquid nitrogen, and stored at −80°C until use. Concentration was determined by Bradford assay and absorbance at 280 nM (extinction coefficient = 1.4).

Binding affinity analysis. The EC_{50} of the MAbs was calculated using ELISA, as described previously (55, 57). Briefly, polystyrene plates (Corning 3690) were coated overnight with 0.5 mg/mL of *wzi50* CPS in PBS, then blocked with 1% PBS-BSA (bovine serum albumin). Antibody was detected using an AP-conjugated goat anti-mouse IgG2b secondary antibody (Southern Biotech, 1091-04, 1:1,000). Control antibodies were run in parallel as negative controls. Binding curves were calculated in GraphPad Prism 6 using a four-parameter variable slope log agonist response curve.

Competitive ELISA. For competitive ELISA, we modified the assay previously described by Banerjee et al. (24). Briefly, 96-well plates were coated overnight at 4°C with 0.5 μg/well of detergent-free purified CPS34 and CPS38. Next, plates were blocked with 2% PBS-BSA for 1 h. After blocking, an antibody cocktail containing one constant anti-CPS MAb at 40 μg/mL and a second competing anti-CPS antibody at increasing concentrations of 0 to 80 μg/mL was added to the coated plates. The decrease in binding affinity to the target CPS was detected by AP-labeled secondary antibodies (1:1,000) against the constant antibody. The competitive binding curve was plotted using GraphPad Prism 6.

***In vitro* whole blood resistance assay.** The *in vitro* whole blood resistance assay was modified from a previously described assay (58) and is described in Methods S3 in Text S1. Briefly, blood samples collected from healthy donors were diluted 1:1 with sterile pre-warmed (37°C) RPMI 1640. Next, 200 μL of the mixture was added to each well of 96-well round-bottomed plates (Becton Dickinson). After this, 1×10^5 CFU per well of bacterial suspensions (MMC34, MMC36, SBU116) was added to blood samples and they were simultaneously treated with either 200 μg of anti-capsular MAbs or isotype controls. At 1 and 2 h, 100 μL of culture was collected and serially plated for CFU/mL quantitation. For all experiments, conditions were performed in triplicate wells, and experiments were all repeated three times.

Macrophage phagocytosis. Macrophage cell line J774A.1 (ATCC) was used for macrophage phagocytosis assays with anti-capsular antibodies using published protocols (24, 29) and as described in the Methods S4 in Text S1. Briefly, 10^6 CFU/well of bacteria was opsonized for 60 min in Dulbecco's Modified Eagle Medium (DMEM) only containing 40 μg/mL of MAb 24D11 or 17H12 and was added at a multiplicity of infection (MOI) = 1 to each well of a 96-well containing 10^6 macrophages per well. For complement-dependent phagocytosis assay, macrophages were treated with 10% normal human serum (NHS) in DMEM. For all experiments, conditions were performed in triplicate wells, and experiments were all repeated three times.

Intratracheal infection of mice. We used C57BL/6 mice (Taconic) aged 6 to 14 weeks for all mouse experiments. Pulmonary infections and analyses of CFU/mL present in collected organs were performed as performed previously (24) and described in the Methods S5 in Text S1.

For pre-opsonized mice, bacterial strains were opsonized with 5 mg/mL of MAb 24D11 for 1 h prior to instilling the opsonized bacteria into the surgically exposed trachea. For the prophylactically treated group, mice were pretreated intraperitoneally with either 100 μL of PBS or 10 mg/kg of MAb 24D11 4 h prior to infecting mice intratracheally with 50 μL of PBS containing 6×10^8 CFU of bacterial inoculum. For the therapeutic group, mice were infected with 50 μL of PBS containing 6×10^8 CFU of bacterial inoculum. Four h post-surgery, they received 10 mg/kg of MAb 24D11 or MAb 17H12 through intraperitoneal injection.

Intratracheal infection of neutropenic mice. To elucidate the efficacy of MAb 24D11 in neutropenic mice, mice were pretreated with 225 μg of rat anti-mouse Ly6G (1A8) or a control rat anti-mouse IgG2a (2A3) (BioXcell) as described previously (29). After 4 h, neutropenic mice received anti-*wzi50* capsular MAbs intraperitoneally, and after 24 h, mice were euthanized, and lung tissues were dissected into two portions. The first halves of the lungs were collected in PBS containing 1$\times$ Pierce Proteinase Inhibitor, serially diluted, and plated on LB agar plates to enumerate CFU. Livers and spleens were processed in 1$\times$ PBS and serially plated for CFU. IL-17 and TNF-α cytokine analyses in lung homogenates were tested using a BioLegend ELISA Max Deluxe set (cat no. 436204 and 430904) according to the manufacturer's protocol.

The remaining portions of lung tissues were processed and labeled for flow cytometry analysis to confirm neutrophil depletion and immunophenotyping, as described in Methods S6 in Text S1. Immune cells were first gated as live/dead cells, followed by CD45$^+$ gating, and then the immune cells were gated as follows: neutrophils (CD45$^+$CD11b$^+$Ly6G$^+$), M1 macrophages (CD45$^+$CD11b$^+$CD11c$^+$F4/80$^+$), M2 macrophages (CD45$^+$CD11b$^+$F4/80$^+$), inflammatory monocytes (CD45$^+$CD11b$^+$Ly6C$^+$Ly6G$^-$), resident monocytes (CD45$^+$CD11b$^+$Ly6C$^-$Ly6G), and T cells (CD45$^+$CD3$^+$) as shown in Fig. S6 in Text S1. All flow cytometry data were processed in BD FACSDiva and Flowing Software (Turku Bioscience, Finland).

Statistical analysis. Statistical tests were performed with GraphPad Prism 6 for Windows. For multigroup comparisons of parametric data (e.g., phagocytosis, serum-resistance assays, and animal experiments), analysis of variance (ANOVA) with *post hoc* analysis using Tukey's, Sidak's, or Dunnett's comparison tests was used. For two-group comparisons of parametric data, we performed paired *t* tests corrected for multiple comparisons using the Holm-Sidak method.

SUPPLEMENTAL MATERIAL

Supplemental material is available online only.

SUPPLEMENTAL FILE 1, PDF file, 1 MB.

ACKNOWLEDGMENTS

We thank Liang Chen and Barry Kreiswirth for gifting us CR-*Kp* strains 33576 and 33576 Δ*wzy* mutant carbapenem-susceptible ST258 *K. pneumoniae* strains (19). We also thank Carol Hill, who with Liang Chen provided in-depth *wzi* data on the strains referenced by van Duin et al. (5). Additionally, we thank Sean Inzerillo for his assistance in testing the binding affinity of MAb 24D11. We thank Esther M. Speer for sharing the whole-blood killing assay protocol with our lab (58). This study was funded using US Veterans Affairs Merit Review Award 5I01 BX003741. B.C.F. is an attending physician at the U.S. Department of Veterans Affairs (Northport VA Medical Center, Northport, NY). The contents of this study do not represent the views of VA or the US government. M.P.M was supported by T32GM008444 and F30 AI140611-01.

K.B., M.P.M., and B.C.F. contributed equally to the ideation and development. B.C.F. oversaw the project. M.P.M. developed the hybridomas and performed vaccinations, splenic fusions, clone screening, subcloning of the hybridomas, and initial purification of the antibody. K.B. was involved in screening the positive clones, assisted with clone screening, and designed and executed all *in vitro* and *in vivo* experiments with the monoclonal antibody, analyzed the data, and generated manuscript figures. C.B.-A., K.B., S.B., R.J., and A.A. were involved in conducting animal experiments and generating *in vivo* data. K.B., M.P.M., C.B.-A., S.B., and B.C.F. contributed equally to writing and editing the manuscript. K.B. and M.P.M. share first co-authorship. Both have written the majority of the manuscript.

We declare that this research was conducted in the absence of any commercial or financial relationships that could be construed as potential conflicts of interest. A patent application has been submitted based on these results by B.C.F., K.B., M.P.M., Stony Brook University, and the U.S. Department of Veterans Affairs (Northport VA Medical Center, Northport, NY).

REFERENCES

1. Rajewsky K. 2019. The advent and rise of monoclonal antibodies. Nature 575:47–49. https://doi.org/10.1038/d41586-019-02840-w.
2. Raj GM, Priyadarshini R, Murugesan S, Adhimoolam M. 2021. Monoclonal antibodies against infectious microbes: so long and too little! Infect Disord Drug Targets 21:4–27. https://doi.org/10.2174/1871526520666200312154649.
3. Parray HA, Shukla S, Perween R, Khatri R, Shrivastava T, Singh V, Murugavelu P, Ahmed S, Samal S, Sharma C, Sinha S, Luthra K, Kumar R. 2021. Inhalation monoclonal antibody therapy: a new way to treat and manage respiratory infections. Appl Microbiol Biotechnol 105:6315–6332. https://doi.org/10.1007/s00253-021-11488-4.
4. Woodford N, Turton JF, Livermore DM. 2011. Multiresistant Gram-negative bacteria: the role of high-risk clones in the dissemination of antibiotic resistance. FEMS Microbiol Rev 35:736–755. https://doi.org/10.1111/j.1574-6976.2011.00268.x.
5. van Duin D, Arias CA, Komarow L, Chen L, Hanson BM, Weston G, Cober E, Garner OB, Jacob JT, Satlin MJ, Fries BC, Garcia-Diaz J, Doi Y, Dhar S, Kaye KS, Earley M, Hujer AM, Hujer KM, Domitrovic TN, Shropshire WC, Dinh A, Manca C, Luterbach CL, Wang M, Paterson DL, Banerjee R, Patel R, Evans S, Hill C, Arias R, Chambers HF, Fowler VG, Jr, Kreiswirth BN, Bonomo RA, Multi-Drug Resistant Organism Network I. 2020. Molecular and clinical epidemiology of carbapenem-resistant Enterobacterales in the USA (CRACKLE-2): a prospective cohort study. Lancet Infect Dis 20:731–741. https://doi.org/10.1016/S1473-3099(19)30755-8.
6. Maraolo AE, Corcione S, Grossi A, Signori A, Alicino C, Hussein K, Trecarichi EM, Viale P, Timsit JF, Veeraraghavan B, Villegas MV, Rahav G, Daikos GL, Vardakas KZ, Roilides E, Uhlemann AC, Ghafur AK, Mornese Pinna S, Bassetti M, Kohler PP, Giacobbe DR. 2021. The impact of carbapenem resistance on mortality in patients with *Klebsiella pneumoniae* bloodstream infection: an individual patient data meta-analysis of 1952 patients. Infect Dis Ther 10:541–558. https://doi.org/10.1007/s40121-021-00408-8.
7. Gomez-Simmonds A, Annavajhala MK, McConville TH, Dietz DE, Shoucri SM, Laracy JC, Rozenberg FD, Nelson B, Greendyke WG, Furuya EY, Whittier S, Uhlemann AC. 2021. Carbapenemase-producing Enterobacterales causing secondary infections during the COVID-19 crisis at a New York City hospital. J Antimicrob Chemother 76:380–384. https://doi.org/10.1093/jac/dkaa466.
8. Gingerich AD, Mousa JJ. 2022. Diverse mechanisms of protective anti-pneumococcal antibodies. Front Cell Infect Microbiol 12:824788. https://doi.org/10.3389/fcimb.2022.824788.
9. Zarei AE, Almehdar HA, Redwan EM. 2016. Hib vaccines: past, present, and future perspectives. J Immunol Res 2016:7203587. https://doi.org/10.1155/2016/7203587.
10. Opoku-Temeng C, Kobayashi SD, DeLeo FR. 2019. *Klebsiella pneumoniae* capsule polysaccharide as a target for therapeutics and vaccines. Comput Struct Biotechnol J 17:1360–1366. https://doi.org/10.1016/j.csbj.2019.09.011.
11. Brisse S, Passet V, Haugaard AB, Babosan A, Kassis-Chikhani N, Struve C, Decre D. 2013. *wzi* Gene sequencing, a rapid method for determination

of capsular type for *Klebsiella* strains. J Clin Microbiol 51:4073–4078. https://doi.org/10.1128/JCM.01924-13.
12. Wang M, Earley M, Chen L, Hanson BM, Yu Y, Liu Z, Salcedo S, Cober E, Li L, Kanj SS, Gao H, Munita JM, Ordoñez K, Weston G, Satlin MJ, Valderrama-Beltrán SL, Marimuthu K, Stryjewski ME, Komarow L, Luterbach C, Marshall SH, Rudin SD, Manca C, Paterson DL, Reyes J, Villegas MV, Evans S, Hill C, Arias R, Baum K, Fries BC, Doi Y, Patel R, Kreiswirth BN, Bonomo RA, Chambers HF, Fowler VG, Arias CA, van Duin D, Multi-Drug Resistant Organism Network I. 2022. Clinical outcomes and bacterial characteristics of carbapenem-resistant Klebsiella pneumoniae complex among patients from different global regions (CRACKLE-2): a prospective, multicentre, cohort study. Lancet Infect Dis 22:401–412. https://doi.org/10.1016/S1473-3099(21)00399-6.
13. Diago-Navarro E, Chen L, Passet V, Burack S, Ulacia-Hernando A, Kodiyanplakkal RP, Levi MH, Brisse S, Kreiswirth BN, Fries BC. 2014. Carbapenem-resistant *Klebsiella pneumoniae* exhibit variability in capsular polysaccharide and capsule associated virulence traits. J Infect Dis 210:803–813. https://doi.org/10.1093/infdis/jiu157.
14. Marsh JW, Mustapha MM, Griffith MP, Evans DR, Ezeonwuka C, Pasculle AW, Shutt KA, Sundermann A, Ayres AM, Shields RK, Babiker A, Cooper VS, Van Tyne D, Harrison LH. 2019. Evolution of outbreak-causing carbapenem-resistant *Klebsiella pneumoniae* ST258 at a tertiary care hospital over 8 years. mBio 10:e01945-19. https://doi.org/10.1128/mBio.01945-19.
15. Satlin MJ, Chen L, Patel G, Gomez-Simmonds A, Weston G, Kim AC, Seo SK, Rosenthal ME, Sperber SJ, Jenkins SG, Hamula CL, Uhlemann AC, Levi MH, Fries BC, Tang YW, Juretschko S, Rojtman AD, Hong T, Mathema B, Jacobs MR, Walsh TJ, Bonomo RA, Kreiswirth BN. 2017. Multicenter clinical and molecular epidemiological analysis of bacteremia due to carbapenem-resistant Enterobacteriaceae (CRE) in the CRE epicenter of the United States. Antimicrob Agents Chemother 61:e02349-16. https://doi.org/10.1128/AAC.02349-16.
16. Wyres KL, Wick RR, Gorrie C, Jenney A, Follador R, Thomson NR, Holt KE. 2016. Identification of *Klebsiella* capsule synthesis loci from whole genome data. Microb Genom 2:e000102. https://doi.org/10.1099/mgen.0.000102.
17. Shropshire WC, Dinh AQ, Earley M, Komarow L, Panesso D, Rydell K, Gomez-Villegas SI, Miao H, Hill C, Chen L, Patel R, Fries BC, Abbo L, Cober E, Revolinski S, Luterbach CL, Chambers H, Fowler VG, Jr, Bonomo RA, Shelburne SA, Kreiswirth BN, van Duin D, Hanson BM, Arias CA. 2022. Accessory genomes drive independent spread of carbapenem-resistant *Klebsiella pneumoniae* clonal groups 258 and 307 in Houston, TX. mBio 13:e0049722. https://doi.org/10.1128/mbio.00497-22.
18. Diago-Navarro E, Motley MP, Ruiz-Perez G, Yu W, Austin J, Seco BMS, Xiao G, Chikhalya A, Seeberger PH, Fries BC. 2018. Novel, broadly reactive anticapsular antibodies against carbapenem-resistant *Klebsiella pneumoniae* protect from infection. mBio 9:e00091-18. https://doi.org/10.1128/mBio.00091-18.
19. Kobayashi SD, Porter AR, Freedman B, Pandey R, Chen L, Kreiswirth BN, DeLeo FR. 2018. Antibody-mediated killing of carbapenem-resistant ST258 *Klebsiella pneumoniae* by human neutrophils. mBio 9:e00297-18. https://doi.org/10.1128/mBio.00297-18.
20. Lang AB, Bruderer U, Senyk G, Pitt TL, Larrick JW, Cryz SJ, Jr. 1991. Human monoclonal antibodies specific for capsular polysaccharides of *Klebsiella* recognize clusters of multiple serotypes. J Immunol 146:3160–3164.
21. Wu MF, Yang CY, Lin TL, Wang JT, Yang FL, Wu SH, Hu BS, Chou TY, Tsai MD, Lin CH, Hsieh SL. 2009. Humoral immunity against capsule polysaccharide protects the host from magA$^+$ *Klebsiella pneumoniae*-induced lethal disease by evading Toll-like receptor 4 signaling. Infect Immun 77:615–621. https://doi.org/10.1128/IAI.00931-08.
22. Seeberger PH, Pereira CL, Khan N, Xiao G, Diago-Navarro E, Reppe K, Opitz B, Fries BC, Witzenrath M. 2017. A semi-synthetic glycoconjugate vaccine candidate for carbapenem-resistant *Klebsiella pneumoniae*. Angew Chem Int Ed Engl 56:13973–13978. https://doi.org/10.1002/anie.201700964.
23. Snitkin ES, Zelazny AM, Thomas PJ, Stock F, Group NCSP, Henderson DK, Palmore TN, Segre JA. 2012. Tracking a hospital outbreak of carbapenem-resistant *Klebsiella pneumoniae* with whole-genome sequencing. Sci Transl Med 4:148ra116. https://doi.org/10.1126/scitranslmed.3004129.
24. Banerjee K, Motley MP, Diago-Navarro E, Fries BC. 2021. Serum antibody responses against carbapenem-resistant *Klebsiella pneumoniae* in infected patients. mSphere 6:e01335-20. https://doi.org/10.1128/mSphere.01335-20.
25. Long SW, Olsen RJ, Eagar TN, Beres SB, Zhao P, Davis JJ, Brettin T, Xia F, Musser JM. 2017. Population genomic analysis of 1,777 extended-spectrum beta-lactamase-producing *Klebsiella pneumoniae* isolates, Houston, Texas: unexpected abundance of clonal group 307. mBio 8:e00489-17. https://doi.org/10.1128/mBio.00489-17.
26. Calzas C, Lemire P, Auray G, Gerdts V, Gottschalk M, Segura M. 2015. Antibody response specific to the capsular polysaccharide is impaired in *Streptococcus suis* serotype 2-infected animals. Infect Immun 83:441–453. https://doi.org/10.1128/IAI.02427-14.
27. Wang Y, Wen Z, Pan X, Briles DE, He Y, Zhang JR. 2018. Novel immunoprotective proteins of *Streptococcus pneumoniae* identified by opsonophagocytosis killing screen. Infect Immun 86:e00423-18. https://doi.org/10.1128/IAI.00423-18.
28. Xiong H, Carter RA, Leiner IM, Tang YW, Chen L, Kreiswirth BN, Pamer EG. 2015. Distinct contributions of neutrophils and CCR2$^+$ monocytes to pulmonary clearance of different *Klebsiella pneumoniae* strains. Infect Immun 83:3418–3427. https://doi.org/10.1128/IAI.00678-15.
29. Motley MP, Diago-Navarro E, Banerjee K, Inzerillo S, Fries BC. 2020. The role of IgG subclass in antibody-mediated protection against carbapenem-resistant *Klebsiella pneumoniae*. mBio 11:e02059-20. https://doi.org/10.1128/mBio.02059-20.
30. D'Andrea MM, Amisano F, Giani T, Conte V, Ciacci N, Ambretti S, Santoriello L, Rossolini GM. 2014. Diversity of capsular polysaccharide gene clusters in Kpc-producing *Klebsiella pneumoniae* clinical isolates of sequence type 258 involved in the Italian epidemic. PLoS One 9:e96827. https://doi.org/10.1371/journal.pone.0096827.
31. Wyres KL, Gorrie C, Edwards DJ, Wertheim HF, Hsu LY, Van Kinh N, Zadoks R, Baker S, Holt KE. 2015. Extensive capsule locus variation and large-scale genomic recombination within the *Klebsiella pneumoniae* clonal group 258. Genome Biol Evol 7:1267–1279. https://doi.org/10.1093/gbe/evv062.
32. Malachowa N, Kobayashi SD, Porter AR, Freedman B, Hanley PW, Lovaglio J, Saturday GA, Gardner DJ, Scott DP, Griffin A, Cordova K, Long D, Rosenke R, Sturdevant DE, Bruno D, Martens C, Kreiswirth BN, DeLeo FR. 2019. Vaccine protection against multidrug-resistant *Klebsiella pneumoniae* in a nonhuman primate model of severe lower respiratory tract infection. mBio 10:e02994-19. https://doi.org/10.1128/mBio.02994-19.
33. Anderluh M, Berti F, Bzducha-Wróbel A, Chiodo F, Colombo C, Compostella F, Durlik K, Ferhati X, Holmdahl R, Jovanovic D, Kaca W, Lay L, Marinovic-Cincovic M, Marradi M, Ozil M, Polito L, Reina JJ, Reis CA, Sackstein R, Silipo A, Švajger U, Vaněk O, Yamamoto F, Richichi B, Vliet SJ. 2021. Recent advances on smart glycoconjugate vaccines in infections and cancer. FEBS J. https://doi.org/10.1111/febs.15909.
34. Doyle CR, Moon JY, Daily JP, Wang T, Pirofski LA. 2018. A capsular polysaccharide-specific antibody alters *Streptococcus pneumoniae* gene expression during nasopharyngeal colonization of mice. Infect Immun 86:e00300-18. https://doi.org/10.1128/IAI.00300-18.
35. Wang Q, Chen Y, Cvitkovic R, Pennini ME, Chang CS, Pelletier M, Bonnell J, Koksal AC, Wu H, Dall'Acqua WF, Stover CK, Xiao X. 2017. Anti-MrkA monoclonal antibodies reveal distinct structural and antigenic features of MrkA. PLoS One 12:e0170529. https://doi.org/10.1371/journal.pone.0170529.
36. Cohen TS, Pelletier M, Cheng L, Pennini ME, Bonnell J, Cvitkovic R, Chang CS, Xiao X, Cameroni E, Corti D, Semenova E, Warrener P, Sellman BR, Suzich J, Wang Q, Stover CK. 2017. Anti-LPS antibodies protect against *Klebsiella pneumoniae* by empowering neutrophil-mediated clearance without neutralizing TLR4. JCI Insight 2:e92774. https://doi.org/10.1172/jci.insight.92774.
37. Pennini ME, De Marco A, Pelletier M, Bonnell J, Cvitkovic R, Beltramello M, Cameroni E, Bianchi S, Zatta F, Zhao W, Xiao X, Camara MM, DiGiandomenico A, Semenova E, Lanzavecchia A, Warrener P, Suzich J, Wang Q, Corti D, Stover CK. 2017. Immune stealth-driven O2 serotype prevalence and potential for therapeutic antibodies against multidrug resistant *Klebsiella pneumoniae*. Nat Commun 8:1991. https://doi.org/10.1038/s41467-017-02223-7.
38. Wang Q, Chang CS, Pennini M, Pelletier M, Rajan S, Zha J, Chen Y, Cvitkovic R, Sadowska A, Heidbrink Thompson J, Yu Lin H, Barnes A, Rickert K, Wilson S, Stover CK, Dall'Acqua WF, Chowdhury PS, Xiao X. 2016. Target-agnostic identification of functional monoclonal antibodies against *Klebsiella pneumoniae* multimeric MrkA fimbrial subunit. J Infect Dis 213:1800–1808. https://doi.org/10.1093/infdis/jiw021.
39. Ahn D, Penaloza H, Wang Z, Wickersham M, Parker D, Patel P, Koller A, Chen EI, Bueno SM, Uhlemann AC, Prince A. 2016. Acquired resistance to innate immune clearance promotes *Klebsiella pneumoniae* ST258 pulmonary infection. JCI Insight 1:e89704. https://doi.org/10.1172/jci.insight.89704.
40. Satlin MJ, Cohen N, Ma KC, Gedrimaite Z, Soave R, Askin G, Chen L, Kreiswirth BN, Walsh TJ, Seo SK. 2016. Bacteremia due to carbapenem-resistant Enterobacteriaceae in neutropenic patients with hematologic malignancies. J Infect 73:336–345. https://doi.org/10.1016/j.jinf.2016.07.002.
41. Chiang MK, Hsiao PY, Liu YY, Tang HL, Chiou CS, Lu MC, Lai YC. 2021. Two ST11 *Klebsiella pneumoniae* strains exacerbate colorectal tumorigenesis in

a colitis-associated mouse model. Gut Microbes 13:1980348. https://doi.org/10.1080/19490976.2021.1980348.
42. Penaloza HF, Noguera LP, Ahn D, Vallejos OP, Castellanos RM, Vazquez Y, Salazar-Echegarai FJ, Gonzalez L, Suazo I, Pardo-Roa C, Salazar GA, Prince A, Bueno SM. 2019. Interleukin-10 produced by myeloid-derived suppressor cells provides protection to carbapenem-resistant *Klebsiella pneumoniae* sequence type 258 by enhancing its clearance in the airways. Infect Immun 87:e00665-18. https://doi.org/10.1128/IAI.00665-18.
43. Casadevall A, Pirofski LA, Joyner MJ. 2021. The principles of antibody therapy for infectious diseases with relevance for COVID-19. mBio 12:03372-20. https://doi.org/10.1128/mBio.03372-20.
44. Motley MP, Fries BC. 2017. A new take on an old remedy: generating antibodies against multidrug-resistant Gram-negative bacteria in a postantibiotic world. mSphere 2:e00397-17. https://doi.org/10.1128/mSphere.00397-17.
45. Casadevall A, Dadachova E, Pirofski LA. 2004. Passive antibody therapy for infectious diseases. Nat Rev Microbiol 2:695–703. https://doi.org/10.1038/nrmicro974.
46. Rivera J, Zaragoza O, Casadevall A. 2005. Antibody-mediated protection against *Cryptococcus neoformans* pulmonary infection is dependent on B cells. Infect Immun 73:1141–1150. https://doi.org/10.1128/IAI.73.2.1141-1150.2005.
47. Nakouzi A, Rivera J, Rest RF, Casadevall A. 2008. Passive administration of monoclonal antibodies to anthrolysin O prolong survival in mice lethally infected with *Bacillus anthracis*. BMC Microbiol 8:159. https://doi.org/10.1186/1471-2180-8-159.
48. Chen T, Blanc C, Liu Y, Ishida E, Singer S, Xu J, Joe M, Jenny-Avital ER, Chan J, Lowary TL, Achkar JM. 2020. Capsular glycan recognition provides antibody-mediated immunity against tuberculosis. J Clin Invest 130:1808–1822. https://doi.org/10.1172/JCI128459.
49. Satlin MJ, Chavda KD, Baker TM, Chen L, Shashkina E, Soave R, Small CB, Jacobs SE, Shore TB, van Besien K, Westblade LF, Schuetz AN, Fowler VG, Jr, Jenkins SG, Walsh TJ, Kreiswirth BN. 2018. Colonization with levofloxacin-resistant extended-spectrum beta-lactamase-producing Enterobacteriaceae and risk of bacteremia in hematopoietic stem cell transplant recipients. Clin Infect Dis 67:1720–1728. https://doi.org/10.1093/cid/ciy363.
50. Satlin M, Hovan M, Westblade L, Calfee DP, Walsh TJ, Kreiswirth BN, Jenkins SG. 2017. Comparison of perianal swab and stool samples for detection of gastrointestinal colonization with ceftriaxone-resistant and fluoroquinolone-resistant Enterobacteriaceae. Open Forum Infect Dis 4:S605–S606. https://doi.org/10.1093/ofid/ofx163.1589.
51. Wright MS, Perez F, Brinkac L, Jacobs MR, Kaye K, Cober E, van Duin D, Marshall SH, Hujer AM, Rudin SD, Hujer KM, Bonomo RA, Adams MD. 2014. Population structure of KPC-producing *Klebsiella pneumoniae* isolates from midwestern U.S. hospitals. Antimicrob Agents Chemother 58:4961–4965. https://doi.org/10.1128/AAC.00125-14.
52. Feldman MF, Mayer Bridwell AE, Scott NE, Vinogradov E, McKee SR, Chavez SM, Twentyman J, Stallings CL, Rosen DA, Harding CM. 2019. A promising bioconjugate vaccine against hypervirulent *Klebsiella pneumoniae*. Proc Natl Acad Sci U S A 116:18655–18663. https://doi.org/10.1073/pnas.1907833116.
53. Bowers JR, Kitchel B, Driebe EM, MacCannell DR, Roe C, Lemmer D, de Man T, Rasheed JK, Engelthaler DM, Keim P, Limbago BM. 2015. Genomic analysis of the emergence and rapid global dissemination of the clonal group 258 *Klebsiella pneumoniae* pandemic. PLoS One 10:e0133727. https://doi.org/10.1371/journal.pone.0133727.
54. Huang SS, Hinrichsen VL, Stevenson AE, Rifas-Shiman SL, Kleinman K, Pelton SI, Lipsitch M, Hanage WP, Lee GM, Finkelstein JA. 2009. Continued impact of pneumococcal conjugate vaccine on carriage in young children. Pediatrics 124:e1–e11. https://doi.org/10.1542/peds.2008-3099.
55. Diago-Navarro E, Calatayud-Baselga I, Sun D, Khairallah C, Mann I, Ulacia-Hernando A, Sheridan B, Shi M, Fries BC. 2017. Antibody-based immunotherapy to treat and prevent infection with hypervirulent *Klebsiella pneumoniae*. Clin Vaccine Immunol 24:e00456-16. https://doi.org/10.1128/CVI.00456-16.
56. Varshney AK, Wang X, Cook E, Dutta K, Scharff MD, Goger MJ, Fries BC. 2011. Generation, characterization, and epitope mapping of neutralizing and protective monoclonal antibodies against staphylococcal enterotoxin B-induced lethal shock. J Biol Chem 286:9737–9747. https://doi.org/10.1074/jbc.M110.212407.
57. Motley MP, Banerjee K, Fries BC. 2019. Monoclonal antibody-based therapies for bacterial infections. Curr Opin Infect Dis 32:210–216. https://doi.org/10.1097/QCO.0000000000000539.
58. Speer EM, Diago-Navarro E, Ozog LS, Dowling DJ, Hou W, Raheel M, Fries BC, Levy O. 2018. Pentoxifylline alone or in combination with gentamicin or vancomycin inhibits live microbe-induced proinflammatory cytokine production in human cord blood and cord blood monocytes *in vitro*. Antimicrob Agents Chemother 62:e01462-18. https://doi.org/10.1128/AAC.01462-18.